Transition Radiation.

Alexander Khanov
Kansas State University, Manhattan, KS
May 1, 2001

Abstract

A thorough review of the transition radiation and its properties will be presented. First, general description of the phenomenon and simple models are given and basic features of the transition radiation are summarized. Then, a brief introduction into the theory of the problem is made. Finally, the experimental applications of the transition radiation are discussed.

1 Transition radiation for freshmen

Transition radiation (TR) is emitted whenever a charged particle traverses the boundary between two media with different optical properties. This effect may be thought of as a result of the reformation of the particle's field when traveling from a medium with dielectric constant, ϵ_1, to a medium with different dielectric constant, ϵ_2. The existence of TR was first suggested by Frank and Ginzburg [1] in 1945.

TR is different from the energy loss of a particle due to its collisions with the atoms. The energy lost due to collisions is emitted by the particle itself and is related to its deceleration. In the case of TR, the radiation occurs even when the particle moves with a constant speed. It is the polarization of the medium which is the source of TR. As a consequence, in the limit of very big particle mass, the energy loss vanishes and TR remains.

TR is similar to another phenomenon called the Cherenkov radiation which occurs when a particle moves with the speed v exceeding the speed of light in the medium ($v > c/n$). Neither effect is related to a particle acceleration, and both stay there for very heavy particles. However, there are important differences. In particular, TR happens for any speed while the Cherenkov radiation has a threshold speed ($v = c/n$) below which there is no effect.

TR can be understood in the following manner [2]. When one looks at an object in an optically dense medium, it appears closer to the surface than it really is. If it moves steadily toward the surface it would appear to move more slowly than it really does. If, then, it manages to continue to move through the surface, then it would appear to accelerate suddenly, and an acceleration is related to a particular radiation emission.

Ginzburg in his Lomonosov Medal laureate lecture [3] mentions other ways to interpret the effect of TR. Let us consider a situation when a charge q comes from a vacuum and falls on a metal that may serve as an ideal mirror. It is known from electrodynamics that the resulting field can be obtained using the method of images, and it is a sum of fields of a charge q moving in the vacuum in the absence of a mirror and a charge $-q$ moving in a mirror to run into q. As soon as the charge crosses the boundary it finds itself in a high-conductivity medium and is unable to produce any field in the vacuum; consequently, the image $-q$ is lost. This process can be interpreted as the charge annihilation, and it results in radiation which is in our case TR.

Yet another interesting model, also mentioned by Ginzburg [3], arises if one considers a medium with periodically changing dielectric constant. For example, if the charge crosses a stack of foils, as it is usually the case in typical TR detectors, it intersects many periodically placed boundaries between air and foils. One may argue (from "the point of view" of a charge) that the charge is subjected to a wave of dielectric permittivity. Scattering of this wave at the charge gives rise to TR. The features of TR (in this model referred to as the transition scattering) can be understood from the analysis of the interference between the original wave (due to the relative motion of the charge and medium) and the scattered (spherical) wave.

2 Basic properties of TR

The basic properties of TR can be understood without involving elaborated theory. I will consider the (most interesting for the practical purposes) ultra relativistic case $\gamma = 1/\sqrt{1 - v^2/c^2} \gg 1$. If TR is uniform in the particle reference frame, from the relativistic transformation to the laboratory reference frame (see [4], Sect. 11.10) it appears that TR is confined in a forward cone of a characteristic angle $\theta_c \sim 1/\gamma$.

Further, TR occurs as a result of the interference between the initial wave (due to the particle motion) and radiated wave (the result of the time-dependent polarization of the medium). Let us consider the transition from vacuum to the dense uniform semi-infinite medium with the index of refraction n. The driving field of the moving particle is proportional to $exp(i\omega t) = exp(i\omega z/v)$ where the z axis is chosen perpendicular to the boundary surface, and generated wave is proportional to $exp(-ikz) = exp[-i\omega(n/c)z]$, so the product is $\sim exp[i\omega z(1/v - n/c)]$. Far from the boundary (for large z) the argument of the exponent quickly oscillates and therefore this region does not contribute to the radiated energy. Significant contribution comes from small z where the phase factor is of the order of unity:

$$\omega z(1/v - n/c) \sim 1 \tag{1}$$

Assuming the frequencies are high enough (above the optical region), the dielectric constant ϵ as a function of frequency ω can be parameterized using the plasma model

$$\epsilon(\omega) = 1 - \omega_p^2/\omega^2 \tag{2}$$

where ω_p is the plasma frequency with typical value for substances with densities of order of unity $\hbar\omega_p \approx 20\ eV$. Substituting to (1) approximations $n = \sqrt{\epsilon} = 1 - \omega_p^2/2\omega^2$ and $1/v = (1 + 1/2\gamma^2)/c$ one gets $z = 2\gamma c/\omega_p(\nu + 1/\nu)$, where $\nu = \omega/\gamma\omega_p$. Following Jackson, I will define the formation length D as $D = max[z(\nu)] = z(\nu = 1)$:

$$D = \gamma c/\omega_p \tag{3}$$

For typical media and $\gamma \sim 10^3$, D is of the order of tens of micrometers.

Typical TR frequency ω_c corresponds to $\nu = 1$, it is

$$\omega_c = \gamma\omega_p \tag{4}$$

Exact calculations show that about half the energy is emitted in the range $0.1 \leq \omega/\omega_c \leq 1$ and the radiation spectrum decreases rapidly for $\omega/\omega_c > 1$.

Finally, let me mention an important formula giving the total energy emitted in TR per interface:

$$I = \frac{1}{3}\alpha\gamma\hbar\omega_p \tag{5}$$

where $\alpha = e^2/\hbar c = 1/137$ is the fine structure constant. Qualitatively (without the factor of 1/3) this result can be obtained *e.g.* within the method of virtual quanta by introducing the minimum relevant transverse scale b_{min} (in our case $b_{min} \sim c/\omega_p$). To an observer at rest at distance b from the particle trajectory, the peak electric field is $E = \gamma e/b^2$ and the pulse time is $\Delta t = b/\gamma c$, so the total energy of the pulse $I \sim E^2 \times \Delta V \sim E^2 b^2 c \Delta t = \gamma e^2/b$. Substituting $b = b_{min}$ one gets $I \sim \alpha\gamma\hbar\omega_p$ [5].

3 Detailed theory of transition radiation

An exact calculation of TR is involved yet quite feasible. The goal is to obtain the TR intensity as a function of frequency and angle. First, let me describe a simplified approach developed in [4], Sect. 13.7.

Let us begin with the electric field of a moving charge. In the particle reference frame, the observer is situated at ρ', $z' = -vt'$ (we are using cylindrical coordinates), and the electric field

$$\begin{aligned} E'_{||}(\mathbf{x}', t') &= -evt'/r'^3 \\ E'_{\perp}(\mathbf{x}', t') &= eb/r'^3 \\ r' &= \sqrt{\rho'^2 + (vt')^2} \end{aligned} \tag{6}$$

In the laboratory reference frame this becomes

$$E_{||}(\mathbf{x},t) = -evt/r^3$$
$$E_{\perp}(\mathbf{x},t) = e\gamma b/r^3 \qquad (7)$$
$$r = \sqrt{\rho^2 + (\gamma vt)^2}$$

The Fourier transform of the field (7) is

$$E_{||}(\mathbf{x},\omega) = -i\sqrt{2/\pi}\frac{ze\omega}{\gamma^2 v^2}e^{i\omega z/v}K_0(\frac{\omega\rho}{\gamma v}) \qquad (8)$$
$$E_{\perp}(\mathbf{x},\omega) = \sqrt{2/\pi}\frac{ze\omega}{\gamma v^2}e^{i\omega z/v}K_1(\frac{\omega\rho}{\gamma v})$$

where K_0, K_1 are modified Bessel functions.

The polarization of the field can be approximately written as

$$\mathbf{P}(\mathbf{x}',\omega) \approx \frac{\epsilon(\omega)-1}{4\pi}\mathbf{E}_i(\mathbf{x}',\omega) \qquad (9)$$

where the initial electric field $\mathbf{E}_i$ is given by equations (8). The radiated field can be then calculated according to the dipole approximation:

$$d\mathbf{E}_{rad} = \frac{e^{ikR}}{R}(\mathbf{k}\times\mathbf{P})\times\mathbf{k}\ d^3x' \qquad (10)$$
$$\mathbf{E}_{rad} = \frac{e^{ikr}}{r}\cdot\frac{\epsilon(\omega)-1}{4\pi}k^2\int_{z'>0}(\hat{\mathbf{k}}\times\mathbf{E}_i)\times\hat{\mathbf{k}}e^{-i\mathbf{k}\cdot\mathbf{x}'}d^3x'$$
$$= \frac{e^{ikr}}{r}\cdot\frac{-\omega_p^2}{4\pi c^2}\int_{z'>0}(\hat{\mathbf{k}}\times\mathbf{E}_i)\times\hat{\mathbf{k}}e^{-i\mathbf{k}\cdot\mathbf{x}'}d^3x'$$

Finally, the TR energy distribution is given by

$$\frac{d^2I}{d\omega d\Omega} = \frac{c}{32\pi^3}(\frac{\omega_p}{c})^4|\int_{z'>0}(\hat{\mathbf{k}}\times\mathbf{E}_i)\times\hat{\mathbf{k}}e^{-i\mathbf{k}\cdot\mathbf{x}'}d^3x'|^2 \qquad (11)$$

The results of calculations can be summarized as the following angular and energy distributions:

$$\frac{d^2I}{d\nu d\eta} \sim \frac{\eta}{\nu^4(1+\frac{1}{\nu^2}+\eta)^2(1+\eta)^2} \qquad (12)$$
$$\frac{dI}{d\nu} \sim (1+2\nu^2)ln(1+\frac{1}{\nu^2})-2$$

Figure 1: Angular distribution of TR at $\nu = 0.1$, $\nu = 1$ and $\nu = 100$ as a function of $\eta = (\gamma\theta)^2$.

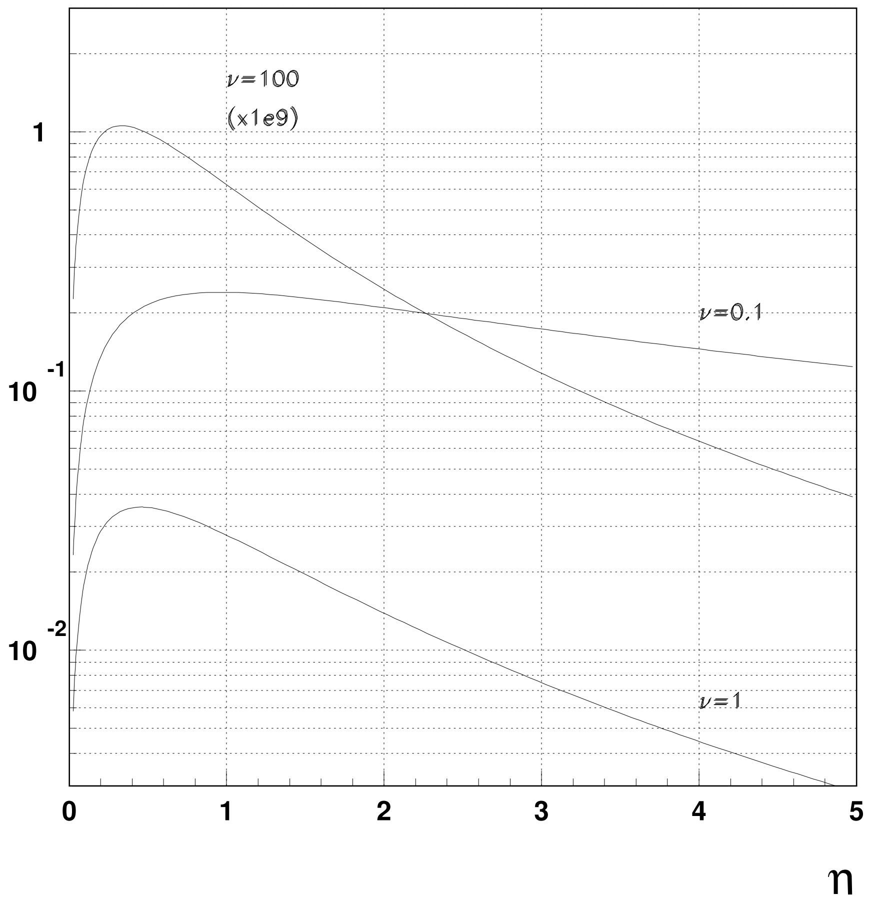

Figure 2: Frequency distribution of TR as a function of $\nu = \omega/\gamma\omega_p$.

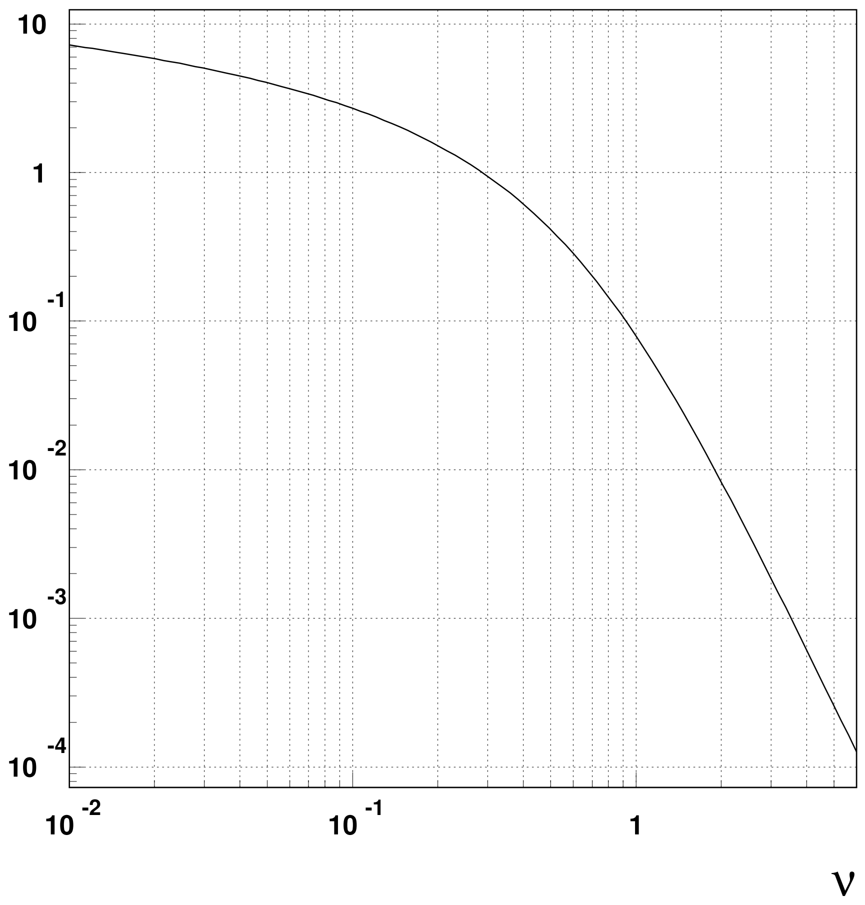

where $\eta = (\gamma\theta)^2,\ \nu = \omega/\gamma\omega_p$. The relevant plots are shown in Figs. 1 and 2.

More elaborated (but much more complicated) approach can be found in [6]. Here I just sketch it very briefly. The idea is to begin with wave equations for a moving charge:

$$\begin{aligned}
\Delta\mathbf{A} - \frac{\hat{\epsilon}}{c^2}\frac{\partial^2\mathbf{A}}{\partial t^2} &= -\frac{4\pi}{c}e\mathbf{v}\delta(\mathbf{r}-\mathbf{v}t) \\
\hat{\epsilon}(\Delta\phi - \frac{\hat{\epsilon}}{c^2}\frac{\partial^2\phi}{\partial t^2}) &= -4\pi e\delta(\mathbf{r}-\mathbf{v}t)
\end{aligned} \tag{13}$$

and perform Fourier transform in t, x, y according to formulae

$$\begin{aligned}
&\mathbf{E}(x,y,z,t) = \int \mathbf{E}_{\omega\mathbf{q}}(z)e^{i(\mathbf{rq}-\omega t)}\frac{d\omega d^2q}{(2\pi)^3} \\
&\mathbf{q} = (k_x, k_y), k_z^2 + q^2 = \epsilon\omega^2/c^2
\end{aligned} \tag{14}$$

and similar expressions for $\mathbf{A}$ and ϕ. The electric field $\mathbf{E}_{\omega\mathbf{q}}$ is found as a sum of initial field $\mathbf{E}^i_{\omega\mathbf{q}}$ and radiated field $\mathbf{E}^{rad}_{\omega\mathbf{q}}$, where initial field is a particular solution of inhomogeneous wave equations (13), and radiated field is the general solution of homogeneous wave equations. The initial field is immediately obtained from the Fourier transform of (13):

$$\begin{aligned}
\phi^i_{\omega\mathbf{q}} &= \frac{4\pi e}{\epsilon v}\frac{e^{i\omega z/v}}{q^2 + \omega^2/v^2 - \epsilon\omega^2/c^2} \\
\mathbf{A}^i_{\omega\mathbf{q}} &= \frac{\epsilon\mathbf{v}}{c}\phi^i_{\omega\mathbf{q}} \\
\mathbf{E}^i_{\omega\mathbf{q}} &= i(\omega\mathbf{v}(\frac{\epsilon}{c^2} - \frac{1}{v^2}) - \mathbf{q})\phi^i_{\omega\mathbf{q}}
\end{aligned} \tag{15}$$

For the radiated field, the longitudinal component can be written as

$$(\mathbf{E}^{rad}_{\omega\mathbf{q}})_z = iae^{\pm ik_z z} \tag{16}$$

with plus sign for the region $z > 0$ ($\epsilon > 1$) and minus sign for the region $z < 0$ ($\epsilon = 1$). The factor a is unknown coefficient to be calculated; it is different for the two regions ($a = a_1$ for $z < 0$ and $a = a_2$ for $z > 0$). The transverse component can be determined from the condition $div\mathbf{D} = 0$, or $\epsilon(\mathbf{q} \pm k_z\mathbf{n})\mathbf{E}^{rad}_{\omega\mathbf{q}} = 0$.

Finally, one can apply boundary conditions (continuous $\epsilon\mathbf{nE}$ and $\mathbf{qE}$), obtain a_1 and a_2, and calculate $d^2I/d\omega d\Omega = 1/4\pi \int \mathbf{E}^2 d^3x$. I will write down the final formula:

$$\frac{d^2 I}{d\omega d\theta} = \frac{e^2 \beta^2 sin^2\theta cos^2\theta}{\pi^2 c(1-\beta^2 cos^2\theta)^2} \left| \frac{(\epsilon - 1)(1-\beta^2 \pm \beta\sqrt{\epsilon - sin^2\theta})}{(1 \pm \beta\sqrt{\epsilon - sin^2\theta})(\epsilon cos\theta + \sqrt{\epsilon - sin^2\theta})} \right|^2 \quad (17)$$

where upper sign corresponds to the case when the particle moves from vacuum to the medium and lower sign corresponds to the opposite case.

4 Practical applications of TR

In many modern high energy physics experiments it is important to separate electrons from heavier particles (pions, protons *etc*). For relatively low energies, this is usually done with Cherenkov detectors which effectively measure the speed of a particle. The momentum of a particle is well known (usually with precision of the order of several percent) from the tracking detectors which measure the bending radius of the particle trajectory in magnetic field. As soon as the momentum $p = mv\gamma$ and the speed v are known, one can calculate the mass.

This method, however, encounters problems as the particle energy becomes very large ($\gamma \gg 1$). One can easily see that the precision in determining the mass $\Delta m/m = \gamma^2 \Delta v/v$. For large γ, the error in m is so large that the particle identification with the Cherenkov detectors becomes impractical, and one needs a detector that measures γ directly.

The TR effect is ideally suited for these purposes, as TR intensity is directly proportional to γ. For high energies, $v \sim 1$ and $m_1/m_2 = \gamma_2/\gamma_1$, so *e.g.* for separation of electrons from pions one gets a factor of $m_\pi/m_e \sim 300$ difference in signal. However, the usage of TR is not straightforward. The main problem can be easily recognized from looking at Eq.(5). Since the average photon energy is of the order of $\hbar\omega_c$ and total emitted energy is $\sim \alpha\hbar\omega_c$, there are only about $\alpha = 1/137$ photons emitted per interface. In other words, the probability to emit a photon is below 1%.

A solution to this problem is to use a set-up with several hundred interfaces, *e.g.* foils or fibres with low Z. One cannot put too many foils in a stack because otherwise the produced photons will be absorbed in the material. The foils can be made thin but not thiner than the formation length (tens of micrometers).

A classical TR detector is composed of several modules, each consisting of a radiator and an x-ray detector, which is usually a multi wire proportional chamber operated with a xenon-rich mixture, in order efficiently to absorb the x-rays. In practice, the signal from TR is always accompanied by the signal due to the ionization. In order to distinguish between these signals, an asymmetric chamber is often used. Any charged particle passing through the TR detector will produce the radiation uniformly across the wire chamber. A high energy electron also produces TR photons, which are preferentially absorbed early in the drift region of the wire chamber. This then gives a large signal at a late time (due to the longer drift distance).

A brief review of the modern TR detectors together with their characteristics is available in the Review of Particle Physics [7]. The TR detectors section (24.4) therein is written by D.Froidevaux who is the leader of the TRT (Transition Radiation Tracker), a part of the ATLAS (A Thoroidal LHC ApparatuS) detector. The ATLAS project is one of the two major detectors to be operated at the Large Hadron Collider at the European Center for Nuclear Research (CERN) in year 2006.

5 Transition Radiation Tracker at ATLAS

Transition Radiation Tracker (TRT) [8] at ATLAS is a large device of 6.8 m length and 206 cm outer diameter. It consists of a radiator (the part where the TR photons are created) and detectors (the wire chambers where the photons are registered). The radiator is made of polypropylene-polyethylene fibres of a very small diameter ($d = 15\ \mu m$) thus providing a lot of interfaces where TR happens. The wire chambers (straw tubes) are made of Kapton and have an internal diameter of 4 mm and a length of 74 cm. They are filled with Xe-rich (70%) gas mixture. Each straw has a single central wire where the signal is collected. The total number of straw tubes in TRT is about 372,000. The schematic view of straws in TRT is shown in Fig. 3.

Unlike many previous TR detectors, TRT is capable of measuring the actual position of a particle track (and therefore its momentum). The detector has 64 layers of the straw tubes (in the central part) which provides very good track position accuracy (50 μm). Dedicated research and development work as well as detailed simulations have shown that the combination of charged-track measurement and particle identification in the same detector will provide a very powerful tool at large luminosities to be achieved at LHC.

The separation of electrons from heavier particles (pions) is illustrated by Figs. 4,5. While the ionization energy from heavier particles has spectrum which quickly goes down for higher energies, the signal from electrons exhibits a long tail that allows their discrimination. The referenced figures show a comparison of between TRT test-beam measurements (dashed lines) and the Photo Absorption Ionization (PAI) Model which was taken as a basis for the detector response simulation.

6 Conclusions

The transition radiation is a very interesting effect that is widely used in high energy physics. In my write-up I did not cover many other aspects of its application. In particular, the TR detectors are used in cosmic ray experiments (to measure energies of muons in the TeV range), in the accelerator physics (to monitor the beam position and shape), in the neutrino experiments *etc.* There are interesting aspects of application of TR in astrophysics, optics, and classical mechanics (for references, see materials following the Ginzburg's lecture in [3]. The last but not the least to say, TR and TR detectors are a subject of many and many dissertations [9].

References

[1] I.Frank, V.Ginzburg, J.Phys. 9 (1945) 353

[2] R.S.Gilmore, Proc. from the SLAC Summer Inst. on Part. Phys., SLAC-R-239 (1980) p.265

[3] V.L.Ginzburg, Usp.Fiz.Nauk 166 (1996) 1033

[4] J.D.Jackson, Classical Electrodynamics (Wiley, New York, 1999, third edition)

[5] M.Zolotorev and K.McDonald http://www.hep.princeton.edu/~mcdonald/accel/weizsacker.ps

[6] L.Landau and E.Lifshitz, Electrodynamics of Continuous Media (Pergamon Press Inc., Oxford, 1985)

[7] D.E.Groom *et al.*, European Phys. J. C15 (2000) 1

[8] T. Akesson *et al.*, Nucl. Instrum. Meth. A412 (1998) 200

[9] http://atlas.web.cern.ch/Atlas/documentation/thesis/thesis.html

Figure 3: Detailed view of straws in TRT.

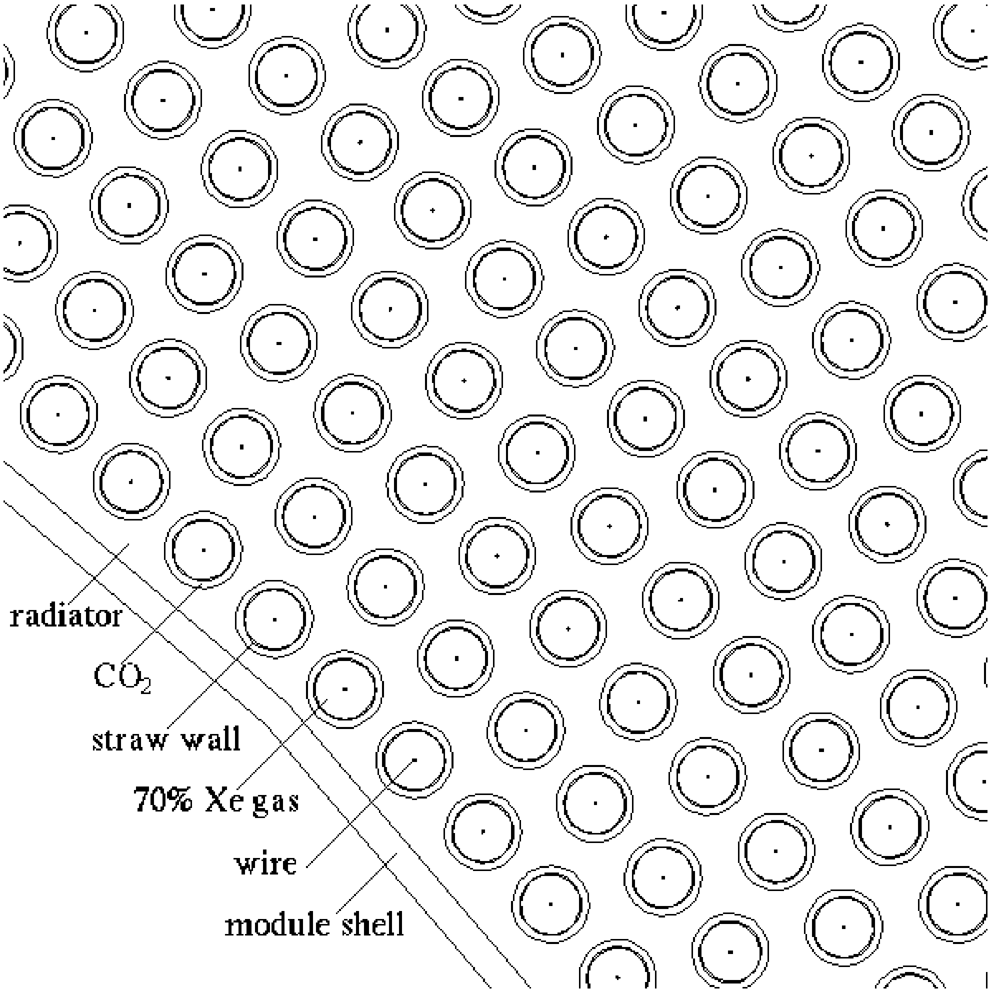

Figure 4: Ionization energy deposition collected on a straw from pions with $p_T = 20\ GeV$.

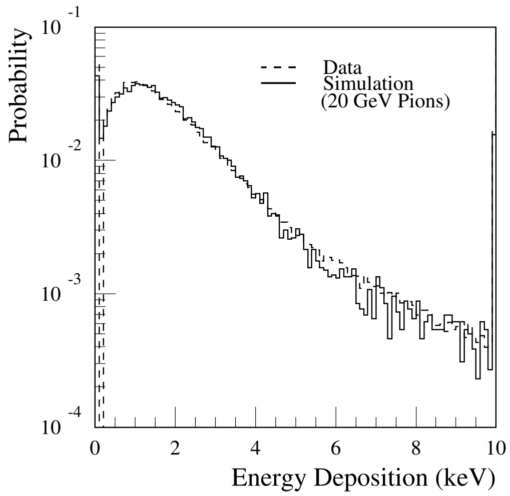

Figure 5: Combined ionization and TR energy deposition collected on a straw from electrons with $p_T = 30\ GeV$.